Experimental realization of a target-accepting quantum search by NMR

Jaehyun Kim, Jae-Seung Lee, and Soonchil Lee
Department of Physics, Korea Advanced Institute of Science and Technology, Taejon 305-701, Korea
(Received 21 June 2001; revised manuscript received 12 November 2001; published 24 April 2002)

With a three-bit nuclear magnetic resonance quantum computer, we have experimentally realized a quantum search algorithm that can take a desired function value (or target) t as its input and give the corresponding function argument x_0 such that $f(x_0)=t$ as a result. The function value is not retrieved from an existing table, but evaluated by the search algorithm in the manner of a typical algorithmic search. A single-query version of the quantum search algorithm is used to search for one of two function arguments.

DOI: 10.1103/PhysRevA.65.054301 PACS number(s): 03.67.Lx

Nuclear magnetic resonance (NMR) has been applied to the experimental realization of a quantum computer giving successful results [1]. Among these experiments, the implementations [2–4] of Grover's search algorithm [5] have attracted attention because this algorithm has practical importance in the sense that many difficult problems in practice can be reduced to search problems. This algorithm assumes an ''oracle'' or a black box that recognizes whether a given item is what we want to find. The complexity or execution time of an oracle is assumed to be a ''unit'' computational step, which is mathematically convenient for the analysis of algorithmic complexity. However, if the quantum oracle is much more complex to realize in practice than a classical oracle, the overall complexity of the quantum algorithm might be greater than that of the classical one. Therefore, all of the elements of a quantum algorithm, including the oracle, should be explicitly implemented when one demonstrates the power of quantum algorithms in practice.

In previous experimental demonstrations [2–4] of the quantum search algorithm, the oracle was implemented by a fixed phase-shift gate, which gives a fixed answer, for example, the third out of four items. In this work, we experimentally realized a quantum search accepting a *target* as its input, using a three-bit NMR quantum computer. The oracle is explicitly implemented in such a way that we can choose the target for which we want to find the argument, contrary to the previous works where the target is fixed. This kind of search is very important in problems where the inverse of a given function is unknown or hard to solve. For this purpose, additional registers are used to represent the function value and target, and an appropriate quantum circuit was implemented, as is well known [6]. We have employed the single-query version [7] of the quantum search algorithm.

A general search problem is finding x_0 such that $F(x_0)=1$ for a given function $F:\{0,1\}^n \mapsto \{0,1\}$, and F is evaluated by an oracle. In the context of the quantum search, the oracle O is equivalently defined as $O|x\rangle=(-1)^{F(x)}|x\rangle$. However, this is the most abstract form and it is important to explicitly implement the oracle when realizing a specific search problem. The detailed structure of the oracle would differ for each case of interest, and here we consider the case where a target is given, i.e., the problem is to find an *index* x_0 such that $f(x_0)=t$ for a given function $f:\{0,1\}^n \mapsto \{0,1\}^m$ and an m-bit target t, which is given arbitrarily.

Since quantum computation works in a reversible way, a search operation S accepting a target is described by

$$S|0\rangle_I|t\rangle_T=|x_0\rangle_I|t\rangle_T, \tag{1}$$

where the subscripts I and T denote the index and target registers, respectively. The initial state of the index register is set by $|0\rangle$ for convenience, and the transformation rule is not specified for the other cases where the initial state is not $|0\rangle$. The conventional description of Grover's algorithm takes only the index state as input. It uses two operators to enhance the probability amplitude of a *marked state* $|x_0\rangle_I$, which is the index state corresponding to a given target. The first operator is the selective phase inversion operator I_t that inverts the sign of only the marked state, i.e.,

$$I_t|x\rangle_I=\pm|x\rangle_I, \tag{2}$$

where the sign is negative when $f(x)=t$ and positive otherwise. The second operator is the inversion about average operator $D=-E+2P$, where E is a unity matrix and $P_{ij}=1/N$ (N is the number of total indices). This operator inverts the amplitudes of all basis states about the mean. Repeated applications of the Grover operator $G=DI_t$ on an equally weighted superposition make the probability amplitude of the marked state close to unity after $O(\sqrt{N})$ cycles.

To implement a quantum search working for an arbitrary target, we used a quantum circuit for I_t that inverts the phase of a state $|x\rangle_I$ if and only if $f(x)=t$ for a given function f and a target t [6]. Since t is not fixed but arbitrary, the essential part of the circuit is the comparison of t with $f(x)$. For comparison, the function is evaluated first in a reversible way by an evaluation operator U_f such that

$$U_f|x\rangle_I|0\rangle_C=|x\rangle_I|f(x)\rangle_C, \tag{3}$$

where the subscript C represents a *content* register, which stores the function values.

If a database, a table of the indices and contents, is given for the search, then U_f is just an addressing scheme retrieving data from the table. Since it is not clear yet how to build an efficient quantum addressing scheme [8], we consider here an *algorithmic* search [6,9] in which the function values are not retrieved from such a table but rather are evaluated by the program code itself. Searching for the extremum of a given function is an example.

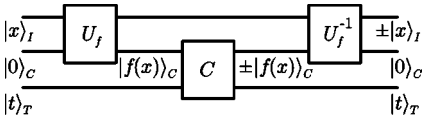

FIG. 1. The quantum network of the extended selective phase inversion operator I_t for the target-accepting search.

Having the quantum circuit for U_f means that we neither already know the answer nor assume fixed solutions, as in the previous experiments. Although U_f has all the information about the function value, the answer is obtained only after execution of a search. For example, one can write a program code evaluating some error function, but having the code, which has all the information about the function, does not mean that it is known which index gives the smallest error. It is still necessary to search for the smallest among the evaluated values.

Once the function has been evaluated, the next step is to compare the contents with the target, via an operator C which inverts the sign of the content register if it matches the target, that is,

$$C|f(x)\rangle_C|t\rangle_T = \pm|f(x)\rangle_C|t\rangle_T, \tag{4}$$

where the sign is negative for $f(x)=t$ and positive otherwise. The execution of CU_f will produce unwanted entanglement between the index and content registers, which must be undone via U_f^{-1} for the algorithm not to fail. Therefore, I_t is realized by [6]

$$I_t = U_f^{-1} C U_f. \tag{5}$$

Thus, the operation of the quantum circuit for the extended I_t on the whole register reads

$$I_t|x\rangle_I|0\rangle_C|t\rangle_T = \pm|x\rangle_I|0\rangle_C|t\rangle_T, \tag{6}$$

as illustrated in Fig. 1. The following implementation of C completes the circuit. Assume that $f(x)$ and t are m-bit binary numbers, and consider a $2m$-bit operator $B=B_1\otimes B_2 \otimes\cdots\otimes B_m$ where B_i is a two-bit operator such that

$$B_i|f^i\rangle_C|t^i\rangle_T = |f^i\rangle_C|\overline{f^i\oplus t^i}\rangle_T, \tag{7}$$

in which f^i and t^i are the ith bits of the content and target registers, respectively. This operator writes 1 on the target register if its inputs are the same, and 0 otherwise. The execution of B makes all the bits of the target register 1 only if the content and target are exactly the same. The result of the comparison can be read using an $(m+1)$-bit Toffoli gate T that takes the target register as control bits and writes the output on an ancillary bit. When the ancilla is prepared in the state $(|0\rangle-|1\rangle)/\sqrt{2}$, the Toffoli gate will invert the sign of the state only if all the bits of the target register are 1. Therefore, C can be implemented by $C=B^{-1}TB$, where B^{-1} is added to restore the original target value t into the target register.

We considered two one-bit functions $f_1(x)=\{0,1\}$ and $f_2(x)=\{1,0\}$ for $x=\{0,1\}$. The remaining two functions $f_3(x)=\{0,0\}$ and $f_4(x)=\{1,1\}$ belong to the cases of no solution or all solution for which any version of Grover's algorithm fails to work. The original version also fails for the case of two items because the inversion about average operation does not enhance the probability amplitude of the marked state but just exchanges those of the two states. However, Chi and Kim's single-query version [7] can be employed in this case. It uses $I_{t\gamma}$ and D_β such that

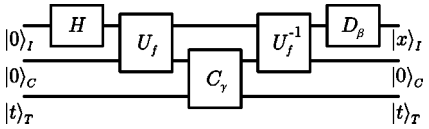

FIG. 2. The whole quantum network for one-bit binary functions.

$$I_{t\gamma}|x\rangle_I = e^{i\gamma}|x\rangle_I, \tag{8}$$

if x is the marked state and does nothing otherwise, and $D_\beta = E+(e^{i\beta}-1)P$. If the number of the marked states m is in the range of $N/4\leqslant m\leqslant N$, then only a single application of $I_{t\gamma}$ followed by D_β gives the answer with $\beta=\gamma=\cos^{-1}(1-N/2m)$. Therefore, this algorithm is applicable to our case where $m=N/2$. Although the quantum search does not show better performance than the classical one for the case of $m=1$, $N=2$, our implementation can be directly extended for $n>2$ cases where this quantum algorithm clearly exhibits superior performance.

The evaluation operators for f_1 and f_2 are given by

$$U_{f_1}=\begin{pmatrix}1&0&0&0\\0&1&0&0\\0&0&0&1\\0&0&1&0\end{pmatrix} \quad \text{and} \quad U_{f_2}=\begin{pmatrix}0&1&0&0\\1&0&0&0\\0&0&1&0\\0&0&0&1\end{pmatrix}, \tag{9}$$

respectively. Since I_t is replaced by $I_{t\gamma}$ in the single-query version, C is also replaced by C_γ, defined by

$$C_\gamma|f(x)\rangle_C|t\rangle_T = e^{i\gamma}|f(x)\rangle_C|t\rangle_T, \tag{10}$$

if $f(x)=t$ and does nothing otherwise. For the $N=2$ and $m=1$ case, both β and γ are $\pi/2$, and

$$C_\gamma = \mathrm{diag}[e^{i\pi/2},1,1,e^{i\pi/2}],$$

$$D_\beta = \begin{pmatrix} e^{i\pi/4} & -e^{-i\pi/4} \\ -e^{-i\pi/4} & e^{i\pi/4}\end{pmatrix}. \tag{11}$$

The whole quantum network is shown in Fig. 2. A Hadamard operator H is used to prepare the initial superposition, and the target state is prepared in $|0\rangle$ or $|1\rangle$ depending on the target value.

In a rotating frame, the NMR Hamiltonian of our three-spin system is given by

$$\mathcal{H} = \sum_i^3 \Delta\omega_i I_{iz} + \sum_{i<j}^3 \pi J_{ij} 2I_{iz}I_{jz}, \tag{12}$$

TABLE I. The preparation sequences and corresponding deviation density operators transformed from the thermal equilibrium state. $J'_{ij}(\theta)$ is equal to $J_{ij}(\theta)I_{kx}(\pi)$, which is simpler to implement in our refocusing scheme.

Sequence	Density operator
No operation	$I_{1z}+I_{2z}+I_{3z}$
$I_{1x}(-\pi/2)J'_{13}(-\pi/2)I_{1y}(\pi/2)$	$2I_{1z}I_{3z}-I_{2z}+I_{3z}$
$I_{1x}(\pi/2)J'_{12}(\pi/2)I_{1y}(\pi/2)$	$2I_{1z}I_{2z}+I_{2z}-I_{3z}$
$I_{3x}(\pi)I_{2x}(-\pi/2)J'_{23}(\pi/2)I_{2y}(\pi/2)$	$-I_{1z}+2I_{2z}I_{3z}-I_{3z}$
$I_{2y}(\pi/2)J'_{12}(\pi/2)J'_{23}(\pi/2)I_{2y}(\pi/2)$	$-I_{1z}-4I_{1z}I_{2z}I_{3z}-I_{3z}$

where $\Delta\omega_i$ and I_{iz} are the chemical shift and z-component angular momentum operator of the spin i, respectively, and J_{ij} is the coupling constant between the spins i and j. This Hamiltonian with rf pulses applied along the x or y axis provides the elementary operators $I_{i\alpha}(\theta)=\exp[-\imath\theta I_{i\alpha}]$ and $J_{ij}(\theta)=\exp[-\imath\theta 2I_{iz}I_{jz}]$, where α is x, y, or z. If we let the spins 1, 2, and 3 represent the index, content, and target registers, respectively, then all the operators in Fig. 2 are expressed as

$$H=I_{1z}(\pi)I_{1y}(-\pi/2),$$

$$U_{f_1}=I_{2y}(\pi/2)I_{1z}(-\pi/2)I_{2z}(-\pi/2)J_{12}(\pi/2)I_{2y}(-\pi/2),$$

$$U_{f_2}=I_{2y}(\pi/2)I_{1z}(-\pi/2)I_{2z}(\pi/2)J_{12}(\pi/2)I_{2y}(-\pi/2),$$

$$C_\gamma=J_{23}(-\pi/2), \text{ and } D_\beta=I_{1x}(-\pi/2),$$

up to the overall phases. U_{f_1} and U_{f_2} are self-inverse. Note that C_γ is implemented by a single operator rather than by the properly modified B and T because such a phase-shift gate is preferable to a Toffoli gate for implementation by the NMR Hamiltonian. Since the content and target registers are one bit each, C_γ can be reduced to a two-qubit phase-shift gate. The initial target state $|0\rangle$ is changed to $|1\rangle$ by applying $I_{3x}(\pi)$ when necessary.

The experiment is performed at room temperature, and thus the spin states are highly mixed in thermal equilibrium state. It is therefore required to convert the thermal equilibrium state into an effective pure state [10–12]. The deviation density operator of the thermal equilibrium state is given by $\rho_{\text{th}}=I_{1z}+I_{2z}+I_{3z}$ and that of the pure state $|000\rangle=|0\rangle_1\otimes|0\rangle_2\otimes|0\rangle_3$ by $\rho_{\text{p}}=I_{1z}+I_{2z}+I_{3z}+2I_{1z}I_{2z}+2I_{2z}I_{3z}+2I_{1z}I_{3z}+4I_{1z}I_{2z}I_{3z}$. ρ_{p} can be produced by subtracting the last density operator from the sum of the first four in Table I. The first column of the table is the optimized preparation sequence used to generate each density operator. We have performed experiments with each preparation sequence to obtain the results expected from the effective pure state.

We used three ^{13}C nuclear spins of 99% carbon-13 labeled alanine in D_2O solvent as qubits. All the experiments were conducted on a Bruker DRX300 spectrometer with proton decoupling. The chemical shifts were measured to be $\Delta\omega_1/2\pi\approx 5979$ Hz, $\Delta\omega_2/2\pi\approx -3476$ Hz, and $\Delta\omega_3/2\pi\approx -6072$ Hz, and the coupling constants J_{12}, J_{23}, and J_{13} were about 54.06 Hz, 34.86 Hz, and -1.30 Hz, respectively. The system was handled in the ''triply rotating'' frame, in which $\Delta\omega_i=0$, i.e., each spin experiences no chemical shifts. Since it was necessary to adjust the phase of each rf pulse controlled in the laboratory frame, the reference phases of the rotating frames were continuously traced by software, which coped with a single reference oscillator for the carbon channel. The operation $I_{iz}(\theta)$ was performed by adjusting the reference phase without any actual rf pulses. The operators $I_{ix(y)}(\pi/2)$ and $I_{ix(y)}(\pi)$ were implemented by the spin-selective UBURP and REBURP pulses [13], respectively, which were about 2 ms in length. During the pulses, there were shifts in the reference phases due to the transient Bloch-Siegert effect [14]. These shifts were carefully measured, and the reference phases were adjusted after each pulse. No hard pulses or multiply selective pulses were used so as to avoid off-resonance [15] and double-resonance two-spin effects [16]. The coupling operator $J_{ij}(\theta)$ was implemented with the refocusing scheme [17–19] optimized for our rotating frame. The experiment took about 16.5 ms in the shortest case and 408.5 ms in the longest, shorter than the shortest spin-spin relaxation time (450 ms) of spin 2.

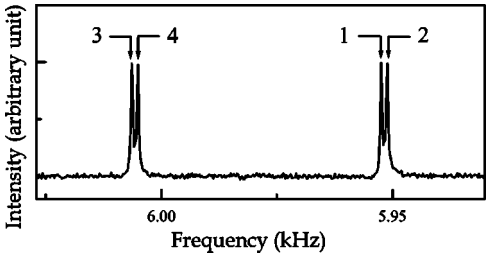

FIG. 3. The reference spectrum of the spin 1 assigned as the index register. The frequency is relative to the resonance frequency 75.475 23 MHz.

Figure 3 shows the reference spectrum of the spin 1, which was assigned as the index register. The large splitting

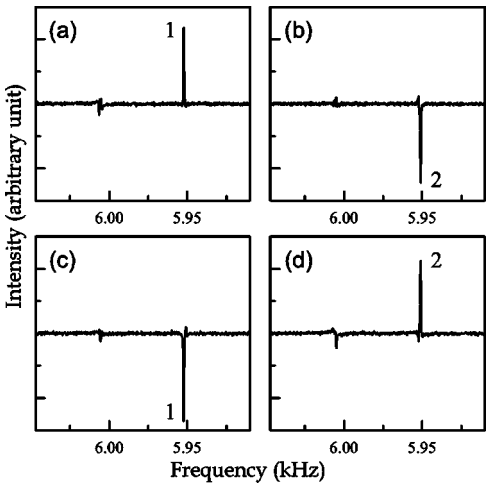

FIG. 4. The result spectra of the spin 1. All the spectra were drawn on the same scale and obtained without any signal averaging. The final state is (a) $|000\rangle$ for f_1 with $t=0$, (b) $|101\rangle$ for f_1 with $t=1$, (c) $|100\rangle$ for f_2 with $t=0$, and (d) $|001\rangle$ for f_2 with $t=1$. The numbers are the labels of the peaks defined in Fig. 3.

is due to the J_{12} coupling and the small to J_{13}. Since $J_{12}>0$ and $J_{13}<0$, the peaks labeled 1, 2, 3, and 4 are observed when spins 2 and 3 are in the states $|00\rangle=|0\rangle_2\otimes|0\rangle_3$, $|01\rangle$, $|10\rangle$, and $|11\rangle$, respectively. Positive absorption peaks represent that spin 1 is in the state $|0\rangle$ and negative peaks, $|1\rangle$. As can be seen in Eq. (6), I_t leaves the initial state unchanged except for the sign of the marked state, and D leaves the state of the content and target registers the same. Since the content register (spin 2) is prepared in the state $|0\rangle$ initially, this means that peaks 3 and 4 are never observed.

The result of the search with the effective pure state shown in Fig. 4 was read by applying a Hadamard operator on the index register. When the given function is f_1 and target is 0, the initial state is $|000\rangle$ and the final state is also $|000\rangle$ because the index corresponding to the target value 0 is 0 for $f_1=\{0,1\}$. This result appears as the positive peak 1, as shown in Fig. 4(a). The spectra in Figs. 4(b), 4(c), and 4(d) clearly show that the final states are $|101\rangle$ for f_1 and $t=1$, $|100\rangle$ for f_2 and $t=0$, and $|001\rangle$ for f_2 and $t=1$, respectively. All the spectra are drawn on the same scale and obtained without any signal averaging. The main reasons for the experimental imperfection are considered to be that the spin-selective pulses could not perfectly suppress the off-resonance effects, and that the spin-spin couplings were not canceled during the applications of pulses.

In summary, we have experimentally implemented quantum searches with a three-bit NMR quantum computer where the index, content, and target registers are one bit each. The target is supplied as an input to be compared with the content, and the accompanying index is given as a result. Chi and Kim's single-query version was used to implement this search for one-bit functions. The experimental results clearly show the answers for given targets.

The authors acknowledge the use of the spectrometer at the Korea Basic Science Institute. This work was supported by the NRL program, Electron Spin Science Center, and the BK21 project.

[1] For recent review, see D.G. Cory, *et al.*, Fortschr. Phys. **48**, 875 (2000); J.A. Jones, *ibid.* **48**, 909 (2000).
[2] J.A. Jones, M. Mosca, and R.H. Hansen, Nature (London) **392**, 344 (1998).
[3] I.L. Chuang, N. Gershenfeld, and M. Kubinec, Phys. Rev. Lett. **80**, 3408 (1998).
[4] L.M.K. Vandersypen *et al.*, Appl. Phys. Lett. **76**, 646 (2000).
[5] L.K. Grover, Phys. Rev. Lett. **79**, 325 (1997).
[6] See, for example, M.A. Nielsen, and I.L. Chuang, *Quantum Computation and Quantum Information* (Cambridge University Press, Cambridge, England, 2000).
[7] D.P. Chi and J. Kim, in *First NASA International Conference on Quantum Computing and Quantum Communications, Palm Springs, 1998*, edited by C.P. Williams (Springer, Berlin, 1998).
[8] C. Zalka, Phys. Rev. A **62**, 052305 (2000).
[9] D. Deutsch and A. Ekert, in *The Physics of Quantum Information: Quantum Cryptography, Quantum Teleportation, Quantum Computation*, edited by D. Bouwmeester, A. Ekert, and A. Zeilinger (Springer, Berlin, 2000).
[10] N. Gershenfeld and I.L. Chuang, Science **275**, 350 (1997).
[11] D.G. Cory, A.F. Fahmy, and T.F. Havel, Proc. Natl. Acad. Sci. U.S.A. **94**, 1634 (1997).
[12] E. Knill, I. Chuang, and R. Laflamme, Phys. Rev. A **57**, 3348 (1998).
[13] H. Geen and R. Freeman, J. Magn. Reson. **93**, 93 (1991).
[14] L. Emsley and G. Bodenhausen, Chem. Phys. Lett. **168**, 297 (1990).
[15] R.R. Ernst, G. Bodenhausen, and A. Wokaun, *Principles of Nuclear Magnetic Resonance in One and Two Dimensions* (Oxford University Press, Oxford, 1987).
[16] E. Kupče, J.-M. Nuzillard, V.S. Dimitrov, and R. Freeman, J. Magn. Reson., Ser. A **107**, 246 (1994); J.-M. Nuzillard and R. Freeman, *ibid.*. **112**, 72 (1995).
[17] N. Linden, B. Hervé, R.J. Carbajo, and R. Freeman, Chem. Phys. Lett. **305**, 28 (1999).
[18] J.A. Jones and E. Knill, J. Magn. Reson. **141**, 322 (1999).
[19] D.W. Leung, I.L. Chuang, F. Yamaguchi, and Y. Yamamoto, Phys. Rev. A **61**, 042310 (2000).